Biomimetic surface topography as a potential modulator of macrophages inflammatory response to biomaterials

N.O. Monteiro, M.R. Casanova, R. Quinteira, J.F. Fangueiro, R.L. Reis, N.M. Neves *

3B's Research Group, I3Bs – Research Institute on Biomaterials, Biodegradables and Biomimetics, Headquarters of the European Institute of Excellence on Tissue Engineering and Regenerative Medicine, University of Minho, AvePark, Parque de Ciência e Tecnologia, Zona Industrial da Gandra, Barco, 4805-017 Guimarães, Portugal
ICVS/3B's–PT Government Associate Laboratory, Braga/Guimarães, Portugal

ARTICLE INFO

ABSTRACT

The implantation of biomaterial devices can negatively impact the local microenvironment through several processes including the injury incurred during the implantation process and the associated host inflammatory response. Immune cell responses to implantable biomaterial devices mediate host-material interactions. Indeed, the immune system plays a central role in several biological processes required for the integration of biomaterials such as wound healing, tissue integration, inflammation, and foreign body reactions. The implant physico-chemical properties such as size, shape, surface area, topography, and chemistry have been shown to provide cues to the immune system. Its induced immune-modulatory responses towards inflammatory or wound healing phenotypes can determine the success of the implant.

In this work, we aim to evaluate the impact of some biomimetic surface topographies on macrophages' acute inflammatory response. For that, we selected 4 different biological surfaces to replicate through soft lithography on spin casting PCL membranes. Those topographies were: the surface of *E. coli*, *S.eppidermidis* and L929 cells cultured in polystyrene tissue culture disks, and an Eggshell membrane. We selected a model based on THP-1-derived macrophages to study the analysis of the expression of both pro-inflammatory and anti-inflammatory markers. Our results revealed that depending on the surface where these cells are seeded, they present different phenotypes. Macrophages present a M1-like phenotype when they are cultured on top of PCL membranes with the surface topography of *E. coli* and *S. epidermidis*. When cultured on membranes with L929 monolayers or Eggshell membrane surface topography, the macrophages present a M2-like phenotype. These results can be a significant advance in the development of new implantable biomaterial devices since they can help to modulate the inflammatory responses to implanted biomaterials by controlling their surface topography.

1. Introduction

One of the major challenges that remain in the conception of implantable biomaterial devices is the understanding of the modulation of the immune response. This response that results from the implantation of the biomaterial device can be crucial for its success [1,2]. An inadequate immune response can lead to several scenarios responsible for the failure of the intervention due to the occurrence of several processes, such as premature reabsorption, fibrous encapsulation and/or implant rejection [3]. Macrophages were reported to have a central role in the immune response to implantable biomaterial devices [4]. As such, these immune cells have been studied to develop immune-modulatory strategies to enhance the success of implantable biomaterial devices. Macrophages are described to have a regulatory function by modulating different functions of other cell types, such as other cells of the immune system [5]. The immune response to the implantable biomaterial devices starts with the recruitment of monocytes to the implant site which leads to its differentiation into macrophages and its posterior adhesion [6]. On the implant site, the activated macrophages release cytokines that recruit other immune cell types involved in the foreign body reaction, which can result in a pro-inflammatory reaction or a wound healing/remodeling scenario [7]. Within these two responses,

macrophages are reported to have different phenotypes that are classically defined as M1 phenotype (pro-inflammatory or classically activated) and M2 phenotype (anti-inflammatory or alternatively activated). Those two different phenotypes are usually distinguished based on the gene expression profile and the cytokines and chemokines released by these immune cells [8].

Several strategies were proposed and developed to modulate the immune response to implantable biomaterial devices [9,10]. They aim to modulate the material-host interaction through the (bio)chemical and physical properties of the implantable material devices. Frequently, they focus on the cell-material interface and involve modifying the surface chemistry, wettability, crystallinity, charge, topography, or stiffness [11,12]. These strategies may also involve functionalization by using coatings or by immobilizing polymers or bioactive molecules on the surface of the implant to mediate the implant-host tissue response. The surface topographies of the implantable biomaterial devices can also influence the macrophage attachment and phenotype, providing opportunities for the modulation of the macrophage function [13–15]. The most common topographies studied are synthetic, such as regular grooves with particular size scales, that have been associated with the M1 or M2 macrophage polarization [16]. However, studies using biomimetic topographies are very scarce in the scientific literature [17,18].

In the present study, we intend to evaluate the effect of different biomimetic topographies on macrophages' M1/M2 polarization. For that, we selected 4 different biological surfaces to be replicated by soft lithography on spin casting PCL membranes. The selection of the topographies intends to be diversified in terms of size ranges and its architecture. As such, we select: 1) the surface topography of monolayers of L929 cells cultured in polystyrene tissue culture disks that intends to evaluate the influence of the surface topography of mammal cells on immune response; 2) the surface topography of Eggshell membrane (ESM) that intends to resemble the surface topography that is typically presented by the extracellular matrix due to its naturally structural fibers; 3) the surface topography of monolayers of *E. coli* cultured in polystyrene tissue culture disks to evaluate if the surface topography this rod-shaped gram – bacteria influences macrophages immune response; 4) the surface topography of monolayers of *S. epidermidis* cultured in polystyrene tissue culture disks to evaluate if the surface topography this cocci gram + bacteria influences macrophages immune response. We intend to replicate with high fidelity these surface topographies on spin-casting Polycaprolactone (PCL) membranes. Polycaprolactone (PCL) was selected as the biomaterial since it is a polymer widely used in implantable biomaterial devices with demonstrated biocompatibility and safety being approved by the Food and Drug Administration (FDA) [19,20]. These properties associated with its thermoplastic character and excellent thermal stability render its suitability for the nanoimprint lithography technique that we used.

The goal of this study was to assess the macrophages' response to the selected natural surface topographies. For that, we selected a model based on THP-1-derived macrophages (dTHP-1) that is widely regarded as a valid model to investigate biomaterials, particularly due to its demonstrated ability to relate to the host response *in vivo* [1,6,7,21–23].

2. Materials and methods

2.1. Preparation of biological templates

For the preparation of L929 monolayers we expand L929 cells - an immortalized mouse lung fibroblast cell line (European Collection of Cell Cultures) - by culturing in Dulbecco's Modified Eagle's medium (DMEM) supplemented with 3.7 g/L sodium bicarbonate, 10 % fetal bovine serum (FBS), and 1 % penicillin–streptomycin. L929 cells were routinely grown in 150 cm^2 culture flasks at 37 °C in a humidified air atmosphere of 5 % CO$_2$ exchanging the medium every 3 days. When cells reached 80 % confluence, cells were detached from the flasks using TrypLE Express (Alfagene, ref. 12605–028), and resuspended in

complete DMEM. Then, the cells were seeded with a density of 30 000 cells on tissue culture polystyrene (TCPS) disks of 13 mm in non-adherent 24 well-plates. When they form a monolayer, cells were washed with PBS and fixed with 10 % formalin and kept at 4 °C. For the preparation of the ESM template (yolk side), the eggshells were soaked in a 10 v/v% of acetic acid solution overnight at room temperature (25 ± 5 °C) to clean and to facilitate the separation of the membrane from the shell. Then, the ESMs were carefully washed with deionized water and the membrane was carefully separated from the shell. After being air-dried at room temperature (25 ± 5 °C), the samples were cut into pieces of 11.5 × 11.5 mm with scissors to be attached to a petri dish with double-sided tape. For the preparation of *E. coli* (ATCC 25922 - LYFO DISK)and *S. epidermidis* (ATCC 35984 - LYFO DISK) monolayers, firstly, using a sterile inoculating loop, bacteria from the stock culture were transferred to tryptic soy broth (TSA) plates and incubated at 37 °C for 18–24 h. From this culture, with a sterile inoculating loop, bacteria are transferred onto 50 mL of fresh tryptic soy broth (TSB) media and grown in a shaking incubator (200 rpm) at 37 °C for 18–24 h. The inoculums were prepared by Sub-culture the cells (1:50 dilution) into 50 mL of fresh TSB and grew for 2 h at 37 °C (200 rpm). The cells were pelleted (2000 rpm, 10 min) and re-suspend the cells in phosphate-buffered saline (PBS pH 7.4). Adjust the cell concentration using a known OD600/ CFU ratio equivalent to 5 × 10^8 CFU/mL (for *E.coli* = 0.4–0.5 and for *S. epidermidis* = 0.5–0.6). Then, cells were seeded on tissue culture polystyrene (TCPS) disks of 13 mm in non-adherent 24 well-plates and grown overnight at 37 °C in a humidified air atmosphere of 5 % CO$_2$. Finally, cells were washed in PBS, fixed with 10 % formalin and kept at 4 °C. (Fig. 1A).

2.2. Production of PDMS negative replicas of the selected biological surfaces

Biological templates (on TCPS or directly in the case of ESM) were attached to double-sided tape and then to a disposable Petri dish with the surface for replication on the upside. Polydimethylsiloxane (PDMS) (SYLGARD 184 Silicone elastomer kit, SCANSCI, DCE-1673921) was prepared according to the manufacturer's instructions. Briefly, the PDMS prepolymer was carefully mixed and cross-linked in a 10: 1 ratio and degassed for 1 h in a vacuum desiccator to remove air bubbles. When pouring the PDMS into Petri dishes containing the respective biological template, any possible bubbles formed could disappear after a few minutes. PDMS was also dispersed in a clean petri dish to originate the template for bare PCL membranes. The PDMS was cured in an oven at 37 °C for 24 h. (Fig. 1B).

2.3. Production of spin casting PCL membranes

A solution of 20 % of polycaprolactone (PCL) (Polycaprolactone- Mn 70,000–90,000 by GPC, Sigma, 440,744) in dichloromethane was homogenized at room temperature (20 ± 5 °C) (Dichloromethane for HPLC, ≥99.8 %, contains amylene as a stabilizer, Laborspirit) until complete homogenization. For the production of the membranes, 1 mL of that solution was dispensed perpendicularly to a glass petri dish (55 mm in diameter) fixed on the Spin Coater (model: WS-650Hzb-23NPPB-UD-3 of Laurell Technologies Corporation) under vacuum. Immediately after the dispensing, the spinning was initiated with the following settings: velocity: 1500 rpm, acceleration: 9300 rpm s^{-1}, time 5 min. After the spinning cycle, the Petri dishes were left in the chemical wood to complete solvent evaporation overnight covered with a needle-perforated aluminum foil.

2.4. Imprinting of biological surface topographies on spin casting PCL membranes

The imprinting of biological templates on the spin-casted PCL membranes was performed by nanoimprint lithography/ hot embossing
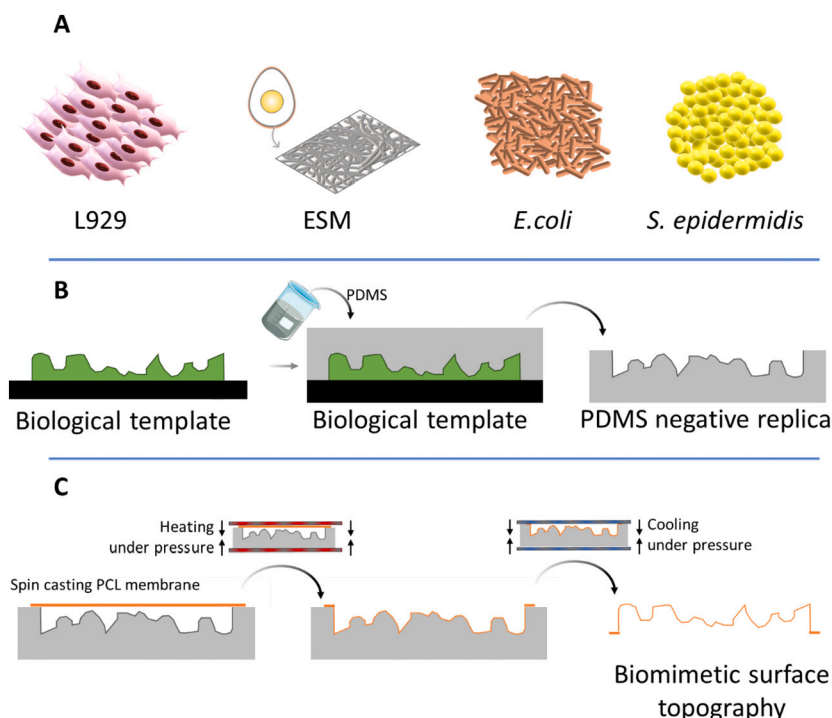
Fig. 1. Schematic representation of the replication of the surface topography of biological templates. A- Biological templates; B- Schematic representation of the production of negative replicas of biological templates; C- Schematic representation of the production of biomimetic PCL membranes by soft lithography.

using a Nanoimprinter (Obducat technologies, Model Eitre 3, Serial number: 003–5095). For that, the PDMS with the negative replicas were placed in contact with the PCL membranes. The imprinting started under a pressure of 3 bar for 30 s with an increase of temperature until 60 °C. After reaching that temperature, the pressure is increased to 5 bar for 1200 s. Finally, the pressure is released, and the set is maintained in contact until it cools down to room temperature. A general explanation of the technique and all the steps involved is depicted in Fig. 1C.

2.5. Atomic force microscopy

For AFM analysis, AFM Dimension Icon (Bruker, USA) was used in PeakForce Tapping (ScanAsyst) mode. The AFM was performed using a silicon nitride tip with a nominal radius of 2 nm (ScanAsyst-Air, Bruker, nominal frequency 70 kHz, nominal spring constant of 0.4 N/m). The linear scanning rate was set between 0.4 and 1 Hz, with a scan resolution of 512 samples per line. Surface roughness analysis was performed on the height images. It is expressed as root mean square roughness (Rq, root mean square average of the roughness profile ordinates) and roughness average (Ra, arithmetic average of the absolute values of the roughness profile ordinates) of height deviations taken from the mean image data plane. The analysis was carried out using commercial AFM software (Bruker). The measurements were performed in the air. Two images from five different samples were taken from each condition.

2.6. Water contact angle

The static contact angles were measured with a Goinometer (Data-Physics Instruments, model OCA 15plus; Germany) at room temperature. The results were achieved by the sessile drop method. For that, 3 μL of water was dispensed through a motor-driven syringe at different zones of each sample. At least ten measurements were carried out for each condition ($n = 10$).

2.7. In vitro assessment

THP-1 cells, a human monocytic cell line, were cultured and expanded in RPMI culture medium (Sigma-Aldrich) supplemented with 1 % penicillin–streptomycin. L929 cells were routinely grown in 150 cm^2 culture flasks at 37 °C in a humidified air atmosphere of 5 % CO2. THP-1 derived macrophages (dTHP-1) were obtained by THP-1 differentiation with 100 nM of phorbol 12-myristate-13-acetate (PMA, Sigma-Aldrich) for 24 h, followed by 24 h cultivation with RPMI PMA-free medium. Non-adhered cells were removed by aspiration and the adherent cells were washed three times with RPMI medium. Then, dTHP-1 were detached from the flasks using TrypLE Express (Alfagene, ref. 12,605–028), and resuspended in complete RPMI. Before the cell seeding on top of the membranes, all membranes were sterilized by soaking them in 70 % ethanol and letting them dry in a sterilized laminar flow chamber. After that, they were exposed to UV light for 30 min on both sides. The cells were seeded on top of the membranes with a density of 100,000 cells per membrane in non-adherent 24 well-plates. Tissue culture polystyrene (TCPS) disks of 13 mm were used as a control. The results were obtained in triplicate in three independent assays.

2.7.1. SEM analysis

SEM was used to analyze the efficacy of the replication of the biological templates surface topography on PCL membranes and both the morphology and attachment of dTHP-1 cultured in the surface membranes. For the samples that contain biological content, cells were fixed with 10 % formalin and kept at 4 °C. Dehydration was performed using a graded series of ethanol concentrations (10 %, 20 %, 40 %, 60 %, 80 %, 90 %, 95 %, and 100 %). Then, the samples were sputter-coated with gold (Fisons Instruments, model SC502; England) for 2 min at 15 mA. Microphotographs were recorded at 5 kV with magnifications of 150× and 1000× by scanning electron microscopy (SEM) (Leica Cambridge, model S360; England).

2.7.2. Immunocytochemistry

Immunocytochemistry was performed after 24 h of the culture of

dTHP-1 on top of PCL membranes. Briefly, cells were fixed in 10 % neutral buffered formalin (ThermoFisher) for 4 h at 4 °C and then washed in PBS. Immunocytochemistry was using a rabbit monoclonal antibody [EPR7854] to Integrin alpha 5 (abcam, diluted 1:100 in 1 % BSA/PBS). Briefly, to block non-specific binding, the samples were incubated with 3 % BSA in PBS, for 30 min at RT. After blocking unspecific binding, primary antibodies were incubated overnight at 4 °C. The next day, cells were washed with PBS and incubated with the secondary antibody Alexa Fluor 488 (against rabbit) (Alfagene; 1:500 diluted in 1 % BSA/PBS) at RT in the dark for 1 h. After several rinses in PBS, phalloidin–tetramethylrhodamine B isothiocyanate (Sigma-Aldrich, diluted 1:1000) and 4,6-Diamidino-2-phenyindole, dilactate (DAPI) were incubated for 30 min in the dark. The images were taken digitally under a fluorescence microscope (Upright Microscope with Thunder, Leica).

2.7.3. RNA isolation and real-time quantitative polymerase chain reaction

After 24 h of culture on top of the PCL membranes, the collected samples were washed with PBS, immersed in Tri reagent® (Life Science, USA), and stored at −80 °C until further use. Total RNA extraction was performed using Tri reagent® method according to the manufacturer's recommendations. The concentration and purity of the extracted RNA were determined using the NanoDrop ND-1000 Spectrophotometer (NanoDrop Technologies Inc., USA). RNA was reverse transcribed into cDNA using the qScript cDNA synthesis kit (Quanta Biosciences, VWR, USA), according to the manufacturer's instructions. Subsequently, the obtained cDNA was used as a template for the amplification of the target genes shown in Table 1, according to the manufacturer's instructions of the PerfeCtaTM SYBR® Green system (Quanta Biosciences, VWR, USA). The qPCR reactions were carried out in a Mastercycler® ep Gradient S realplex® thermocycler (Eppendorf; Germany).

Glyceraldehyde-3-phosphate-dehygrogenase (GAPDH) was used as the reference gene, and the expression of all target genes was normalized to the expression of this housekeeping gene for the same sample. The gene expression quantification was performed according to the Livak method ($2^{-\Delta\Delta CT}$ method), considering the TCPS (negative control) as a calibrator.

2.7.4. Analysis of the cytokines and chemokines released

Supernatants from each sample of the *in vitro* experiments were collected and stored at −80 °C. 24 h before multiplex analysis, samples were transferred to −20 °C and then to 4 °C. The samples were analyzed with Invitrogen's Inflammation 20-Plex Human ProcartaPlex™ Panel (#EPX200–12185-901) and read on the Luminex MAGPIX system. The results presented in a heat map were normalized to the mean value of cytokine/chemokine quantified on the bare condition. In the supplementary figure is presented the data expressed in pg mL^{-1}. See Table 2

Table 2
List of pro- and anti-inflammatory cytokines and chemokines analyzed.

Phenotype	Acronym	Full name
Pro-inflammatory	E-Selectin	E-Selectin
	GM-CSF	Granulocyte-macrophage colony-stimulating factor
	IFN-γ	Interferon-gamma
	IL-1α	Interleukin-1 alpha
	IL-1β	Interleukin-1 beta
	IL-12p70	Interleukin-12p70
	IL-17A	Interleukin-17A
	IL-6	Interleukin-6
	IL-8	Interleukin-8
	IP-10	Interferon gamma-induced protein-10
	MCP-1	Monocyte chemoattractant protein-1
	MIP-1α	macrophage inflammatory protein-1 alpha
	MIP-1β	macrophage inflammatory protein-1 beta
	P-Selectin	P-Selectin
	sICAM-1	Soluble intercellular adhesion molecule-1
	TNF-α	Tumor necrosis factor-alpha
Anti-inflammatory	IFN-α	Interferon-alpha
	IL-10	Interleukin-10
	IL-13	Interleukin-13
	IL-4	Interleukin-4

for the list of pro-and anti-inflammatory cytokines that were analyzed.

3. Results

We used as biological templates: 1) the surface topography of monolayers of the fibroblast cell line L929 cultured in polystyrene tissue culture disks; 2) the surface topography of the Eggshell membrane (ESM); 3) the surface topography of monolayers of *E. coli* cultured in polystyrene tissue culture disks; 4) the surface topography of monolayers of *S. epidermidis* cultured in polystyrene tissue culture disks. (Fig. 1A). In the left row of Fig. 2 it is presented SEM micrographs of the biological templates that were used. We observed that L929 cells formed a complete monolayer when cultured in TCPS. ESM presents a fibrillar-like structure, similar to what is presented by the native extracellular matrix of connective tissues. *E. coli* distribute randomly among all the TCPS surfaces, being observed a formation of large colonies. *S. epidemidis* distribute among the TCPS surface, forming colonies that clearly do not form a monolayer but allow these bacteria to form multiple layers on top of TCPS. To replicate the surface of these biological templates, we first used a replica molding rapid fabrication technique to obtain a negative replica of the biological surfaces on PDMS. PDMS is a flexible silicone elastomer, that is commonly used in soft lithography techniques (Fig. 1B). Besides the biological templates, we also replicated

Table 1
Primer sequences used for RT-PCR procedures[a].

Gene	Forward (5′-3′)	Reverse (5′-3′)
GAPDH	CAACTCCCTCAAGATTGTCAGCAA	GGCATGGACTGTGGTCATGA
TNFα	ATGTTGTAGCAAACCCTCAAGC	TGATGGCAGAGAGGAGGTTG
IL-6	AGGAGACTTGCCTGGTGAAA	GCATTTGTGGTTGGGTCAG
IL-1β	TGAGCTCGCCAGTGAAATGA	AGGAGCACTTCATCTGTTTAGGG
CXCL-9	GATTGGAGTGCAAGGAACCC	TAGTCCCTTGGTTGGTGCTG
CXCL-10	TTCTGAGCCTACAGCAGAGGA	GGTACTCCTTGAATGCCACTTAGA
NOS2	GGACATCGCGTGGGTGAA	TTTATCGCTCGGAGCCTGC
IL-4	GCACCGAGTTGACCGTAACA	AGGAATTCAAGCCCGCCAG
ARG-1	GGAAAACCAAGTGGGAGCAT	TGTGGTTGTCAGTGGAGTGT
IL-10	AAGACCCAGACATCAAGGCG	AATCGATGACAGCGCCGTAG
SIGLEC-1	CAACTTGCTGCGTGTGGAGA	TGCCTGATTAGATCCTCCTCGG
MRC-1	TGCTCTACAAGGGATCGGGT	ACACGCCAAACAAGAACATGA

[a] GAPDH = glyceraldehyde 3-phosphate dehydrogenase;. ARG-1 = Human arginase-1; MRC-1 = Human mannose receptor C-type 1; SIGLEC-1 = Human sialic acid binding Ig like lectin 1; NOS2 = Human nitric oxide synthase 2; IL-10 = Human interleukin 10; IL-6 = Human interleukin 6; TNFα = Human tumor necrosis factor; IL-4 = Human interleukin 4; IL-1β = Human interleukin 1 beta; CXCL9 = Human C-X-C motif chemokine ligand 9; CXCL10 = Human C-X-C motif chemokine ligand 10.
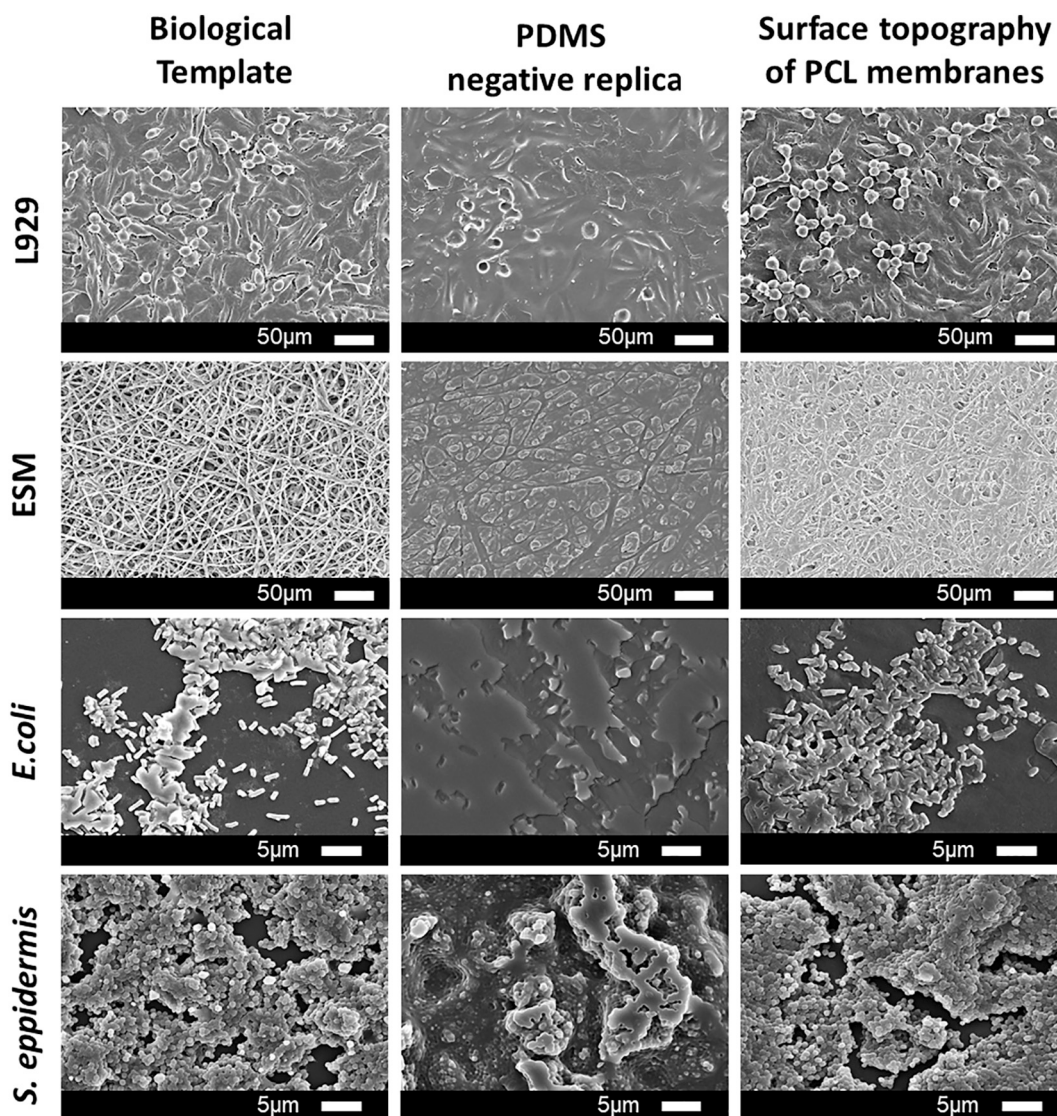
Fig. 2. SEM micrographs of biological templates (left row), PDMS negative replicas (middle row) and surface topography of produced PCL membranes (right row).

a flat surface (that was used as a negative control) under the same processing conditions. To transfer these surface topographies to PCL, firstly, spin casting PCL membranes were fabricated that were flexible, homogeneous, and with a mean thickness of 0.5 ± 0.1 mm. Secondly, the soft lithography technique was applied to imprint surfaces of all PDMS replicas on spin-casting PCL membranes. In the end, it was obtained: 1) bare PCL membranes; 2) PCL membranes with the biomimetic surface topography of monolayers of L929 cells (bL929); 3) PCL membranes with the biomimetic surface topography of ESM (bESM); 4) PCL membranes with the biomimetic surface topography of *E.coli* cultured on top of TCPS (bEC); 5) PCL membranes with the biomimetic surface topography *of S. epidemidis* cultured on top of TCPS (bSE) (Fig. 2 - middle row). A schematic overview of the main steps to achieve the final topography on PCL membranes is presented in Fig. 1.

The analysis of success and the fidelity of replication of the selected topographies was assessed by SEM analysis. In Fig. 2 it is represented the native surface of the biological templates that were used as well as the PDMS negative replica and its replication on the PCL membranes (left, middle and right rows respectively). The success of the replication method was performed by comparing both images for each type of template. We observe that the structure of the surface topography presented by biological templates it is very similar to the structure that was imprinted on the correspondent PCL membrane. We achieved the

replication of the details of the surface until the nanoscale (see fig. S1 on supplementary material). This allows us to call them biomimetic surface topographies. "Table 3 presents the analysis of both roughness and wettability (assessed by AFM and water contact angle, respectively) of the produced PCL membranes. Analyzing all the conditions differences are noticed in both roughness and wettability between them, in which bare (control) presents the lowest value of average roughness (Ra) and bSE presents the highest. Thus, the roughness varies as bSE > bESM > bL929 > bEC > bare. The same variation is observed for the water contact angle values.".

SEM micrographs allow us to analyze the attachment of dTHP-1 to the various produced PCL membranes after 24 h in culture, without a

Table 3
Characterization of the roughness and wettability parameters of the produced PCL membranes.

| Sample	Roughness average (nm)	Water contact angle (°)
bL929	218.5 ± 89.8	97.9 ± 6.0
bESM	263.0 ± 45.5	116.0 ± 5.2
bEC	14.8 ± 2.6	88.3 ± 4.3
bSE	432.5 ± 59.1	126.4 ± 5.8
Bare	13.9 ± 3.5	$87,4 \pm 5.0$

significant difference in terms of cell morphology (Fig. 3A). Immuno-cytochemistry analysis confirms that dTHP-1 cells do not present significant differences regarding their morphology after 24 h of culture on top of different substrates analyzed. Moreover, in all analyzed conditions, dTHP-1 cells express α5 Integrin, a protein involved in the formation of focal adhesions and cell attachment.

A gene expression analysis of immunomodulatory markers expressed by dTHP-1 was performed (Fig. 4). The analysis of those immunomodulatory genes can be subdivided in two categories: 1) the genes that are typically expressed by macrophages with a M1-like phenotype (TNF-α, IL-6, IL-1β, CXCL-9, CXCL-10 and NOS2) and 2) the genes that are typically expressed by macrophages with a M2-like phenotype (IL-4, Arg-1, IL-10, Siglec-1 and MRC). No significant differences were observed in the expression of the analyzed biomarkers between the conditions where dTHP-1 were cultured on top of TCPS and Bare PCL membranes. dTHP-1 cultured on top of bL929 present a significatively lower expression of genes IL-6, IL-1β and CXCL-9 that are typically associated with the M1 phenotype of these cells when compared with dTHP-1 cultured on both TCPS and/or bare PCL membrane. Moreover, compared with dTHP-1 cultured on top of both TCPS and/or bare PCL membrane, these cells on bL929 present a significant increase of the expression of genes IL-4, Arg-1, Siglec-1 and MRC that are typically associated with the M2 phenotype of macrophages. Similar to the previously described condition, dTHP-1 cultured on top of bESM present a significative lower expression of genes IL-6, IL-1β and CXCL-9 that are typically associated with the M1 phenotype of these cells when compared with dTHP-1 cultured on both TCPS and/or bare PCL membrane. Additionally, by comparison with dTHP-1 cultured on top of both TCPS and/or bare PCL membrane, these cells on bESM present a significant increase of the expression of genes IL-4, Arg-1, Siglec-1 and MRC that are usually associated with the M2 phenotype of macrophages. dTHP-1 cultured on top of bEC present a significative higher expression of genes TNF-α, CXCL-10 and NOS2 that are usually associated with the M1 phenotype of these cells when compared with dTHP-1 cultured on both TCPS and/or bare PCL membrane. Moreover, compared with dTHP-1 cultured on top of both TCPS and/or bare PCL membrane, these
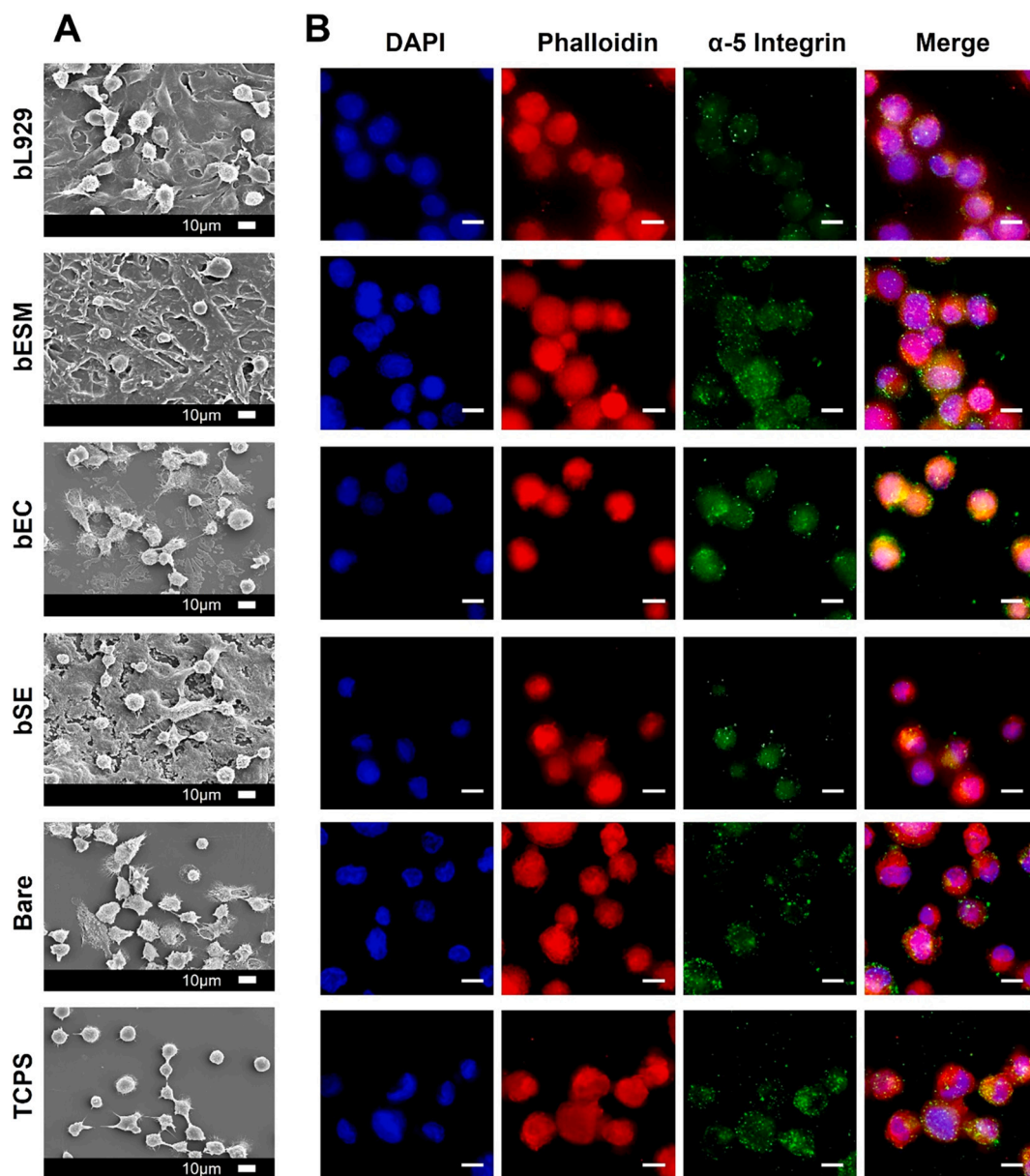
Fig. 3. dTHP1 on top of all analyzed substrates after 24 h of culture. A- SEM micrographs of dTHP-1 on top of all analyzed substrates; B- Immunofluerencence analysis of dTHP-1 on top of all analyzed substrates (blue- DAPI; Red- phalloidin–tetramethylrhodamine B isothiocyanate; Green- α-5 integrin) (scale bar 10 μm).
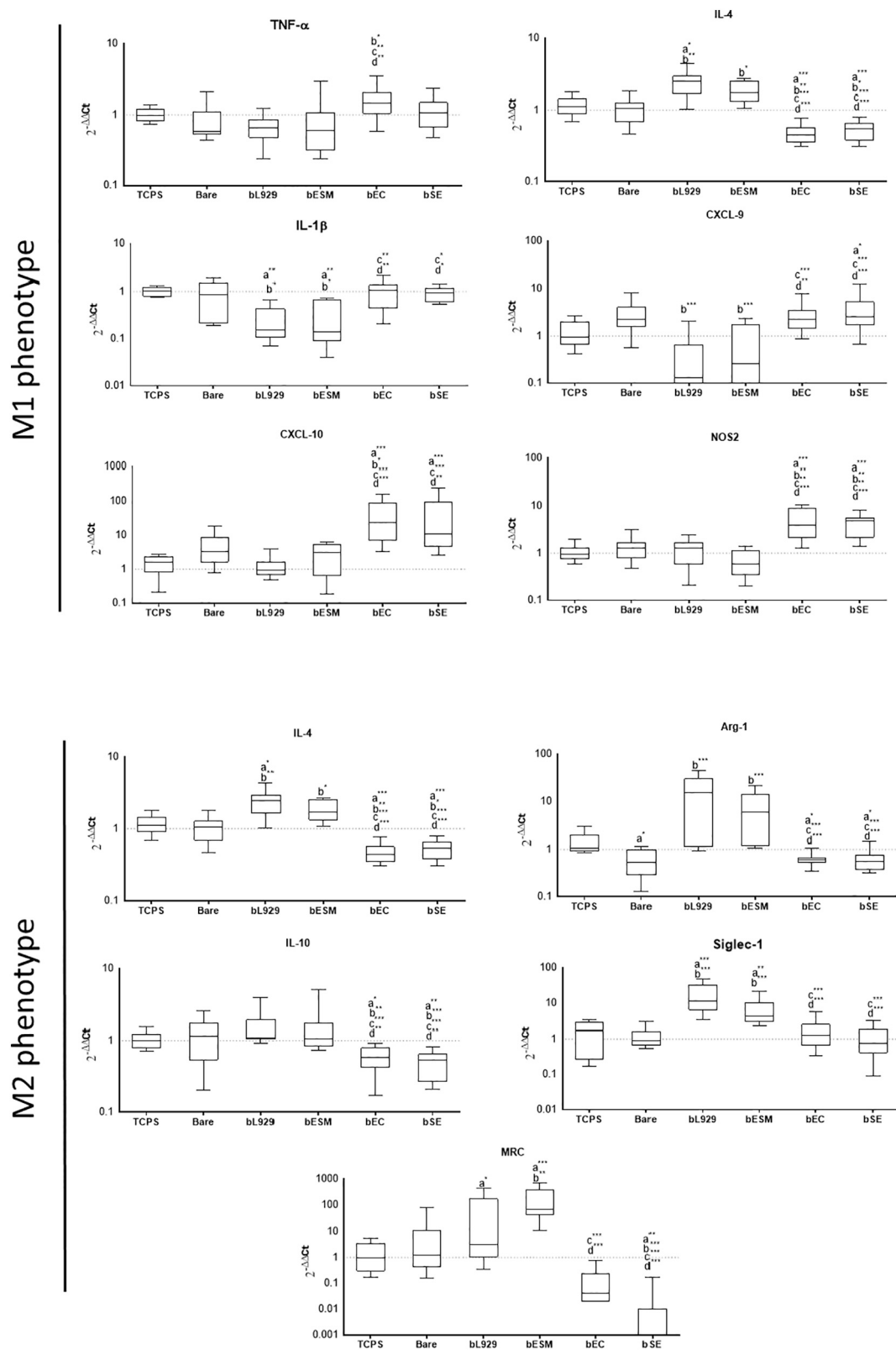
Fig. 4. Relative expression of immunomodulatory markers by dTHP-1. The expression was normalized against the GAPDH gene and the quantification was performed according to the Livak method, considering the control condition (TCPS) as calibrator. Data were analyzed by the Kruskal-Wallis test, followed by the Tukey's HSD test ($p < 0.01$): a denotes significant differences compared to TCPS, b denotes significant differences compared to Bare, c denotes significant differences compared to bL929 and d denotes significant differences compared to bESM; *p < 0.01; **p < 0.001; ***p < 0.0001.

cells on bEC present a significative lower expression of genes IL-4, Arg-1 and IL-10 that are typically associated with the M2 phenotype of macrophages. Parallel to the previously described condition dTHP-1 cultured on top of bSE present a significative higher expression of genes IL-6, CXCL-9, CXCL-10 and NOS2 that are typically associated with the M1 phenotype of these cells when compared with dTHP-1 cultured on both TCPS and/or bare PCL membrane. Furthermore, compared with dTHP-1 cultured on top of both TCPS and/or bare PCL membrane, these cells on bSE present a significative lower expression of genes IL-4, Arg-1, IL-10 and MRC that are normally associated with the M2 phenotype of macrophages.

An extensive analysis of 20 biomarkers released by dTHP-1 during 24 h in culture on top of all studied surfaces revealed that these cells present different release profiles when cultured on top of different substrates with different surface topographies (Figs. 5 and S2). The heat map (Fig. 5) presents the normalized values of the quantification of chemokines/cytokines released by dTHP-1 cultured on top of biomimetic PCL membranes compared with the average quantification of these inflammatory markers released by dTHP-1 on top of bare PCL membranes. It is possible to observe that the release profile of chemokines/cytokines by dTHP-1 is similar to the conditions where these cells were cultured on top of bL929 and on top of bESM. In these two conditions, we observe a higher content of chemokines/cytokines that are typically associated with the M2 phenotype of macrophages and a lower content of chemokines/cytokines that are typically associated with the M1 phenotype. It is also possible to observe that the release profile of chemokines/cytokines by dTHP-1 cultured on top of bEC and bSE is similar. In these two conditions, we observe a higher content of chemokines/cytokines that are typically associated with the M1 phenotype of macrophages and a lower content of chemokines/cytokines that are typically associated with the M2 phenotype.
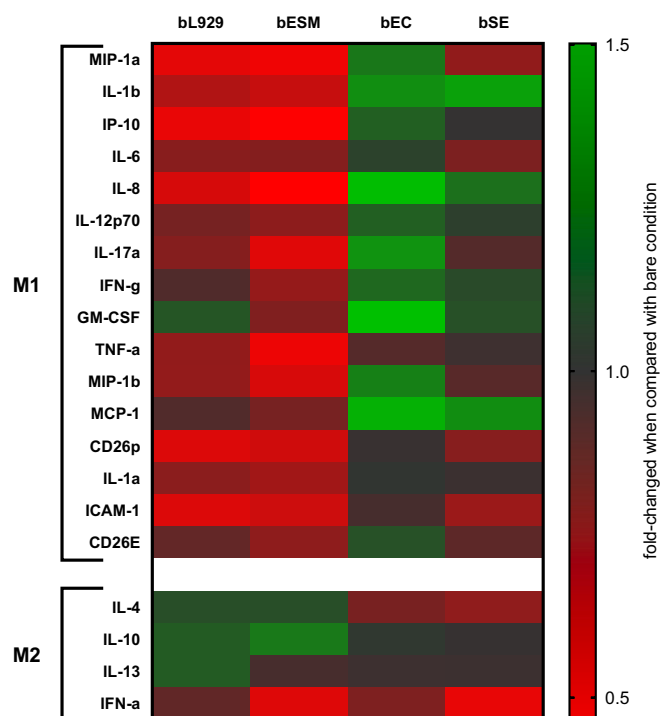

Fig. 5. Heat map representation of the relative immunomodulatory cytokines and chemokines released by dTHP-1. The results presented were achieved by dividing the mean value of cytokine/chemokine quantified by those of the bare condition. Full results obtained by the quantification of cytokines and chemokines released by dTHP-1 are presented in Fig. S2.

4. Discussion

Considerable efforts have been made to provide better integration between the host tissues and implantable biomaterial devices, avoiding a rejection caused by an exacerbated immune response [3]. The design of implantable devices that can modulate the immune response to avoid those negative reactions is a huge challenge still today [18]. In this work, we tested the ability of biomimetic surface topographies that can easily be imprinted on biomaterials to modulate the immune response [17,18]. For that, we selected four different biological surface topographies. The selection intends to mimic the surface of animal cells (bL929), the extracellular matrix (bESM), and bacteria surfaces (bEC and bSE). These topographies were replicated on PCL membranes by soft lithography with high fidelity (Fig. 2). We were able to replicate the surface topography of mammal cells (monolayers of L929 cells cultured in polystyrene tissue culture disks); the surface topography of Eggshell membrane (ESM) that intends to resemble the surface topography that is typically presented by the extracellular matrix due to its naturally structural fibers; the surface topography rod-shaped gram – bacteria (monolayers of *E. coli* cultured in polystyrene tissue culture disks) and the surface topography of monolayers of cocci gram + bacteria (*S. epidermidis* cultured in polystyrene tissue culture disks).

Aiming to assess the macrophages' response to the selected surface topographies, we selected a model based on dTHP-1 that is a valid model to predict the host response *in vivo* [1,6,7,21–23]. dTHP-1 do not present significant differences in its morphology when cultured on top of all analyzed substrates. The mechanisms that underlie the polarization of macrophages in response to the substrate topography are yet to be fully elucidated. Our results revealed a ubiquitous expression of α5-Integrin by dTHP-1 in all analyzed conditions (Fig. 3). This protein is involved in the formation of focal adhesions necessary forsubsequent cell adhesion [24]. Nevertheless, further studies comprising the analysis of expression of other integrins and other adhesion-associated proteins could contribute to elucidate this mechanism. As such, follow-up studies may consider evaluating specifically which of those proteins are involved in the signal transduction that results in the M1/M2 polarization of macrophages. Indeed, Integrin α2β1 [25], Integrin αv β 5 [26] and integrin α2β3 [27] were previously reported to have a direct effect on macrophage phenotype by inducing the polarization of macrophages into M2 phenotype. Studies comprising the blocking of these adhesion-associated proteins with antibodies (high specificity) or even its silencing with siRNAs can be developed to elucidate the mechanisms that underlie the macrophages' response obtained in the present work.

The analysis of the gene expression of inflammatory-related markers (Fig. 4) was conducted considering nine different genes. Between those nine genes, six of them are related to a macrophage pro-inflammatory like phenotype: TNF-α [28], IL-6 [29], IL-1β [28,30], CXCL-9 [31], CXCL-10 [31] and NOS2 [32,33]. The remaining five genes are related to a healing inflammation like phenotype of macrophages: IL-4 [34], Arg-1 [30], IL-10 [34], siglec-1 [30] and MRC [30]. In this analysis, we did not observe significant differences between the expression of these genes in the condition where dTHP-1 were cultured on top of TCPS and on top of Bare PCL membranes. These results revealed that there is no induction of the development of a specific inflammation of these cells by the different surface chemistry of PCL *versus* the surface chemistry of TCPS. Nevertheless, when dTHP-1 are cultured on top of PCL membranes with the imprinted biomimetic surface topographies, the profile of expression of the analyzed genes revealed significant differences. Looking in detail on this analysis, it was observed that both bL929 and bESM conditions presented a similar gene expression profile, with a significant underexpression of IL-6, IL-1 and CXCL-9 biomarkers and a significative overexpression of IL-4, Arg-1 [35–37], Siglec-1 and MRC biomarkers by comparison with those cells that were cultured on top of bare PCL membranes. This can be an indicator that, when macrophages are in contact with these kinds of surface topographies, they present a M2 like phenotype. It is also observed that in the condition bEC the gene

expression profile of dTHP-1 present a significative overexpression of TNF-α, CXCL-10 and NOS2 biomarkers and a significative under expression of IL-4, and IL-10 biomarkers when compared to those cells cultured on top of bare PCL membranes. The cells cultured on top of bSE present a significative overexpression of the NOS2 biomarker and a significative under expression of IL-4, IL-10 and MRC biomarkers, by comparison of the gene expression presented by those cells cultured on top of bare PCL membranes. These results suggest that, when macrophages are placed in contact with biomimetic surface topographies of bacteria, they are more prone to develop a pro-inflammatory response. Interestingly, NOS2 is over expressed in both bEC and bSE conditions. NOS2 is associated with macrophage response to bacterial infection, suggesting that the recognition of the surface topography of bacteria can be an important trigger for the activation of NOS2 signaling pathway leading to an inflammatory response [32,33].

In the analysis of the release profile of inflammatory biomarkers, it was considered the analysis of 20 different biomarkers (Figs. 5 and S2). Overall, P-selectin, *E*-selectin and ICAM-1 are correlated with the promotion of cell adhesion, in this particular case, to the implantable material, and the other analyzed markers are associated with the interplay of immune cells to develop an immune response [21,38,39]. Of the 20 analyzed markers, 16 of them are typically associated with the macrophage's M1-like phenotype and the remaining 4 (IL-4 [34], IL-10 [34], IL-13 and IFN-α) are related to macrophage's M2-like phenotype [39]. Once again, the results revealed that, when cultured on top of bL929 and bESM, dTHP-1 present a higher value of anti-inflammatory associated markers and a lower value of pro-inflammatory associated markers. This profile is typically presented by M2-like polarized macrophages, by comparison of the release profile of these cells cultured on bare PCL membranes. When those cells are cultured on top of bEC and bSE they present higher values of pro-inflammatory associated markers and a lower value of anti-inflammatory associated markers. This profile is typically presented by M1-like polarized macrophages, by comparison to the release profile of these cells cultured on bare PCL membranes. Those results suggest that the selected surface topographies can be used to modulate the immune response.

5. Conclusions

Several strategies to modulate the immune system using biomaterials properties, including surface topography were investigated. Our study provides important new findings in demonstrating that biological surface topographies inspired by mimicking the extracellular matrix, bacteria surface and mammalian cells surface can generate different immune responses in macrophages. Herein, we demonstrated the ability of the selected topographies to promote an anti- or pro-inflammatory response by the genetic markers associated with the phenotypes M1 or M2, respectively. The surface topography of biomaterials can have paramount importance to tune the immune response developed by biomaterial devices. This opens new avenues for personalized implantable biomaterial devices with a modulated response of the immune system.

CRediT authorship contribution statement

N.O. Monteiro: Conceptualization, Methodology, Validation, Formal analysis, Investigation, Writing – original draft, Writing – review & editing, Visualization. **M.R. Casanova:** Methodology, Validation, Formal analysis, Investigation, Writing – review & editing, Visualization. **R. Quinteira:** Methodology, Validation, Investigation, Writing – review & editing. **J.F. Fangueiro:** Conceptualization, Validation, Formal analysis, Investigation, Writing – review & editing, Visualization, Supervision. **R.L. Reis:** Writing – review & editing, Resources, Funding acquisition. **N.M. Neves:** Conceptualization, Supervision, Writing – review & editing, Resources, Funding acquisition.

Declaration of competing interest

The authors declare that they have no known competing financial interests or personal relationships that could have appeared to influence the work reported in this paper.

Data availability

Data will be made available on request.

Appendix A. Supplementary data

Supplementary data to this article can be found online at https://doi.org/10.1016/j.bioadv.2022.213128.

References

[1] S. Segan, M. Jakobi, P. Khokhani, S. Klimosch, F. Billing, M. Schneider, D. Martin, U. Metzger, A. Biesemeier, X. Xiong, A. Mukherjee, H. Steuer, B.M. Keller, T. Joos, M. Schmolz, U. Rothbauer, H. Hartmann, C. Burkhardt, G. Lorenz, N. Schneiderhan-Marra, C. Shipp, Systematic investigation of polyurethane biomaterial surface roughness on human immune responses in vitro, Biomed. Res. Int. 2020 (2020), https://doi.org/10.1155/2020/3481549.

[2] I.T. Swinehart, S.F. Badylak, Extracellular matrix bioscaffolds in tissue remodeling and morphogenesis, Dev. Dyn. 245 (2016) 351–360, https://doi.org/10.1002/dvdy.24379.

[3] A. Crupi, A. Costa, A. Tarnok, S. Melzer, L. Teodori, Inflammation in tissue engineering: the Janus between engraftment and rejection, Eur. J. Immunol. 45 (2015) 3222–3236, https://doi.org/10.1002/eji.201545818.

[4] J.M. Anderson, A. Rodriguez, D.T. Chang, Foreign body reaction to biomaterials, Semin. Immunol. 20 (2008) 86–100, https://doi.org/10.1016/j.smim.2007.11.004.

[5] L. Davenport Huyer, S. Pascual-Gil, Y. Wang, S. Mandla, B. Yee, M. Radisic, Advanced strategies for modulation of the material-macrophage interface, Adv. Funct. Mater. 30 (2020) 1–21, https://doi.org/10.1002/adfm.201909331.

[6] K.R. Fernandes, Y. Zhang, A.M.P. Magri, A.C.M. Renno, J.J.J.P. Van Den Beucken, Biomaterial property effects on platelets and macrophages: an in vitro study, ACS Biomater. Sci. Eng. 3 (2017) 3318–3327, https://doi.org/10.1021/acsbiomaterials.7b00679.

[7] J. Li, Y.J. Zhang, Z.Y. Lv, K. Liu, C.X. Meng, B. Zou, K.Y. Li, F.Z. Liu, B. Zhang, The observed difference of macrophage phenotype on different surface roughness of mineralized collagen, Regen. Biomater. 7 (2020) 203–211, https://doi.org/10.1093/RB/RBZ053.

[8] A. Mantovani, A. Sica, S. Sozzani, P. Allavena, A. Vecchi, M. Locati, The chemokine system in diverse forms of macrophage activation and polarization, Trends Immunol. 25 (2004) 677–686, https://doi.org/10.1016/j.it.2004.09.015.

[9] E.M. Moore, D.R. Maestas, H.Y. Comeau, J.H. Elisseeff, The immune system and its contribution to variability in regenerative medicine, Tissue Eng.B Rev. 27 (2021) 39–47, https://doi.org/10.1089/ten.teb.2019.0335.

[10] B.N. Brown, S.F. Badylak, The Role of the Host Immune Response in Tissue Engineering And Regenerative Medicine, Fourth Ed., Elsevier, 2013 https://doi.org/10.1016/B978-0-12-398358-9.00025-2.

[11] E. Mariani, G. Lisignoli, R.M. Borzì, L. Pulsatelli, Biomaterials: foreign bodies or tuners for the immune response? Int. J. Mol. Sci. 20 (2019) https://doi.org/10.3390/ijms20030636.

[12] R.M. Boehler, J.G. Graham, L.D. Shea, Tissue engineering tools for modulation of the immune response, Biotechniques. 51 (2011) 239–254, https://doi.org/10.2144/000113754.

[13] P.C.S. Bota, A.M.B. Collie, P. Puolakkainen, R.B. Vernon, E.H. Sage, B.D. Ratner, P. S. Stayton, Biomaterial topography alters healing in vivo and monocyte/macrophage activation in vitro, J. Biomed. Mater. Res. A 95 A (2010) 649–657, https://doi.org/10.1002/jbm.a.32893.

[14] N.E. Paul, C. Skazik, M. Harwardt, M. Bartneck, B. Denecke, D. Klee, J. Salber, G. Zwadlo-Klarwasser, Topographical control of human macrophages by a regularly microstructured polyvinylidene fluoride surface, Biomaterials 29 (2008) 4056–4064, https://doi.org/10.1016/j.biomaterials.2008.07.010.

[15] H. Cao, K. Mchugh, S.Y. Chew, J.M. Anderson, The topographical effect of electrospun nanofibrous scaffolds on the in vivo and in vitro foreign body reaction, J. Biomed. Mater. Res.A 93 (2010) 1151–1159, https://doi.org/10.1002/jbm.a.32609.

[16] S. Chen, J.A. Jones, Y. Xu, H.Y. Low, J.M. Anderson, K.W. Leong, Characterization of topographical effects on macrophage behavior in a foreign body response model, Biomaterials 31 (2010) 3479–3491, https://doi.org/10.1016/j.biomaterials.2010.01.074.

[17] A. Lock, J. Cornish, D.S. Musson, The role of in vitro immune response assessment for biomaterials, J. Funct. Biomater. 10 (2019), https://doi.org/10.3390/jfb10030031.

[18] E. Antmen, N.E. Vrana, V. Hasirci, The role of biomaterials and scaffolds in immune responses in regenerative medicine: macrophage phenotype modulation by biomaterial properties and scaffold architectures, Biomater. Sci. 9 (2021) 8090–8110, https://doi.org/10.1039/d1bm00840d.

[19] E.R. Balmayor, I. Pashkuleva, A.M. Frias, H.S. Azevedo, R.L. Reis, Synthesis and functionalization of superparamagnetic poly-ε- caprolactone microparticles for the selective isolation of subpopulations of human adipose-derived stem cells, J. R. Soc. Interface 8 (2011) 896–905, https://doi.org/10.1098/rsif.2010.0531.

[20] N.O. Monteiro, J.F. Fangueiro, N.M. Neves, Fabrication of biomimetic patterned PCL membranes mimicking the complexity of Rubus fruticosus leaves surface, Colloids Surf.B Biointerfaces (2021), 111910, https://doi.org/10.1016/j.colsurfb.2021.111910.

[21] Y. Liu, W. Deng, L. Yang, X. Fu, Z. Wang, P. Van Rijn, Q. Zhou, T. Yu, Biointerface topography mediates the interplay between endothelial cells and monocytes, RSC Adv. 10 (2020) 13848–13854, https://doi.org/10.1039/d0ra00704h.

[22] M.A. Alfarsi, S.M. Hamlet, S. Ivanovski, Titanium surface hydrophilicity modulates the human macrophage inflammatory cytokine response, J. Biomed. Mater. Res.A 102 (2014) 60–67, https://doi.org/10.1002/jbm.a.34666.

[23] H.S. Lee, S.J. Stachelek, N. Tomczyk, M.J. Finley, R.J. Composto, D.M. Eckmann, Correlating macrophage morphology and cytokine production resulting from biomaterial contact, J. Biomed. Mater. Res. A 101 A (2013) 203–212, https://doi.org/10.1002/jbm.a.34309.

[24] O.J. Mezu-Ndubuisi, A. Maheshwari, The role of integrins in inflammation and angiogenesis, Pediatr. Res. 89 (2021) 1619–1626, https://doi.org/10.1038/s41390-020-01177-9.

[25] B.H. Cha, S.R. Shin, J. Leijten, Y.C. Li, S. Singh, J.C. Liu, N. Annabi, R. Abdi, M.R. Dokmeci, N.E. Vrana, A.M. Ghaemmaghami, A. Khademhosseini, Integrin-mediated interactions control macrophage polarization in 3D hydrogels, Adv. Healthc. Mater. 6 (2017) 1–12, https://doi.org/10.1002/adhm.201700289.

[26] Q. Yao, J. Liu, Z. Zhang, F. Li, C. Zhang, B. Lai, L. Xiao, N. Wang, Peroxisome proliferator-activated receptor γ (PPARγ) induces the gene expression of integrin αvβ5 to promote macrophage M2 polarization, J. Biol. Chem. 293 (2019) 16572–16582, https://doi.org/10.1074/jbc.RA118.003161.

[27] H. Wang, R.T.T. Morales, X. Cui, J. Huang, W. Qian, J. Tong, W. Chen, A photoresponsive hyaluronan hydrogel nanocomposite for dynamic macrophage immunomodulation, Adv. Healthc. Mater. 8 (2019) 1–9, https://doi.org/10.1002/adhm.201801234.

[28] G.S. Ashcroft, M.J. Jeong, J.J. Ashworth, M. Hardman, W. Jin, N. Moutsopoulos, T. Wild, N. McCartney-Francis, D. Sim, G. McGrady, X.Y. Song, S.M. Wahl, Tumor necrosis factor-alpha (TNF-α) is a therapeutic target for impaired cutaneous wound healing, Wound Repair Regen. 20 (2012) 38–49, https://doi.org/10.1111/j.1524-475X.2011.00748.x.

[29] J. Mauer, J.L. Denson, J.C. Brüning, Versatile functions for IL-6 in metabolism and cancer, Trends Immunol. 36 (2015) 92–101, https://doi.org/10.1016/j.it.2014.12.008.

[30] A. Vinhas, A.F. Almeida, A.I. Gonçalves, M.T. Rodrigues, M.E. Gomes, Magnetic stimulation drives macrophage polarization in cell to–cell communication with Il-1β primed tendon cells, Int. J. Mol. Sci. 21 (2020) 1–15, https://doi.org/10.3390/ijms21155441.

[31] A. Engström, A. Erlandsson, D. Delbro, J. Wijkander, Conditioned media from macrophages of M1, but not M2 phenotype, inhibit the proliferation of the colon cancer cell lines HT-29 and CACO-2, Int. J. Oncol. 44 (2014) 385–392, https://doi.org/10.3892/ijo.2013.2203.

[32] K. Bian, F. Ghassemi, A. Sotolongo, A. Siu, L. Shauger, A. Kots, F. Murad, NOS-2 signaling and cancer therapy, IUBMB Life 64 (2012) 676–683, https://doi.org/10.1002/iub.1057.

[33] J. Braverman, S.A. Stanley, Nitric oxide modulates macrophage responses to Mycobacterium tuberculosis infection through activation of HIF-1α and repression of NF-κB, J. Immunol. 199 (2017) 1805–1816, https://doi.org/10.4049/jimmunol.1700515.

[34] N. Makita, Y. Hizukuri, K. Yamashiro, M. Murakawa, Y. Hayashi, IL-10 enhances the phenotype of M2 macrophages induced by IL-4 and confers the ability to increase eosinophil migration, Int. Immunol. 27 (2015) 131–141, https://doi.org/10.1093/intimm/dxu090.

[35] Z. Yang, X.F. Ming, Functions of arginase isoforms in macrophage inflammatory responses: impact on cardiovascular diseases and metabolic disorders, Front. Immunol. 5 (2014) 1–10, https://doi.org/10.3389/fimmu.2014.00533.

[36] M. Rath, I. Müller, P. Kropf, E.I. Closs, M. Munder, Metabolism via arginase or nitric oxide synthase: two competing arginine pathways in macrophages, Front. Immunol. 5 (2014) 1–10, https://doi.org/10.3389/fimmu.2014.00532.

[37] J.T. Pesce, T.R. Ramalingam, M.M. Mentink-Kane, M.S. Wilson, K.C.E. Kasmi, A.M. Smith, R.W. Thompson, A.W. Cheever, P.J. Murray, T.A. Wynn, Arginase-1-expressing macrophages suppress Th2 cytokine-driven inflammation and fibrosis, PLoS Pathog. 5 (2009), https://doi.org/10.1371/journal.ppat.1000371.

[38] J. Suzuki, E. Hamada, T. Shodai, G. Kamoshida, S. Kudo, S. Itoh, J. Koike, K. Nagata, T. Irimura, T. Tsuji, Cytokine secretion from human monocytes potentiated by P-selectin-mediated cell adhesion, Int. Arch. Allergy Immunol. 160 (2013) 152–160, https://doi.org/10.1159/000339857.

[39] S.N. Randeria, G.J.A. Thomson, T.A. Nell, T. Roberts, E. Pretorius, Inflammatory cytokines in type 2 diabetes mellitus as facilitators of hypercoagulation and abnormal clot formation, Cardiovasc. Diabetol. 18 (2019) 1–16, https://doi.org/10.1186/s12933-019-0870-9.